

Modulating the Therapeutic Activity of Nanoparticle Delivered Paclitaxel by Manipulating the Hydrophobicity of Prodrug Conjugates

Steven M. Ansell,^{*,†} Sharon A. Johnstone,[†] Paul G. Tardi,[†] Lily Lo,[†] Sherwin Xie,[†] Yu Shu,[†] Troy O. Harasym,[†] Natasha L. Harasym,[†] Laura Williams,[†] David Bermudes,[†] Barry D. Liboiron,[†] Walid Saad,[‡] Robert K. Prud'homme,[‡] and Lawrence D. Mayer[†]

Celator Pharmaceuticals Corporation, 1779 West 75th Avenue, Vancouver, B.C., V6P 6P2, Canada, and Department of Chemical Engineering, Princeton University, Princeton, New Jersey

Received January 2, 2008

A series of paclitaxel prodrugs designed for formulation in lipophilic nanoparticles are described. The hydrophobicity of paclitaxel was increased by conjugating a succession of increasingly hydrophobic lipid anchors to the drug using succinate or diglycolate cross-linkers. The prodrugs were formulated in well defined block copolymer-stabilized nanoparticles. These nanoparticles were shown to have an elimination half-life of approximately 24 h in vivo. The rate at which the prodrug was released from the nanoparticles could be controlled by adjusting the hydrophobicity of the lipid anchor, resulting in release half-lives ranging from 1 to 24 h. The diglycolate and succinate cross-linked prodrugs were 1–2 orders of magnitude less potent than paclitaxel in vitro. Nanoparticle formulations of the succinate prodrugs showed no evidence of efficacy in HT29 human colorectal tumor xenograph models. Efficacy of diglycolate prodrug nanoparticles increased as the anchor hydrophobicity increased. Long circulating diglycolate prodrug nanoparticles provided significantly enhanced therapeutic activity over commercially formulated paclitaxel at the maximum tolerated dose.

Introduction

In recent years there has been increasing interest in chemotherapeutic treatment regimes involving multiple drugs. Recent evidence from our laboratory has revealed that many drug combinations act synergistically when exposed at appropriate ratios and antagonistically at other ratios in cell based studies.^{1–4} One of the problems encountered when translating these findings to in vivo studies is that the exposed drug ratio changes over time because of the different pharmacokinetic behavior of the individual drugs when administered in a conventional aqueous based cocktail. To address this issue, we have developed liposome-based delivery systems that maintain drug ratios at synergistic levels in vivo through coordinated release of the drugs.^{1–4} Although liposomes are adequate delivery vehicles for hydrophobic compounds, they are predominantly designed for water soluble drugs. Hydrophobic drugs typically dissolve in the liposome bilayer where they are subject to facile exchange processes when exposed to hydrophobic sinks such as lipoproteins or cells in the blood compartment after in vivo administration.⁵ As a result, development of alternative delivery technologies is being pursued that are compatible with both hydrophobic and hydrophilic drugs and allow the simultaneous control of the rates at which drugs are made bioavailable.

The drug delivery approach applied here was to combine two well-known concepts, namely, the use of prodrugs and the utilization of micellar or nanoparticle delivery vehicles to facilitate pharmacokinetic control of hydrophobic drugs such as paclitaxel. The goal of most prodrug technologies is typically to make hydrophobic drugs more hydrophilic for increased solubility in an aqueous environment.⁶ However, when such drugs are made more hydrophobic and consequently more

compatible with lipid based delivery systems, it is possible to adjust the properties of two disparate drugs such that their effective release rates in vivo are matched. Micelles or lipophilic nanoparticle carriers can be used to suspend these prodrugs in aqueous environment because the individual drugs themselves are otherwise insoluble.

Parameters that are likely to affect the in vivo availability of a drug when optimizing the design of such systems include (1) the plasma elimination of the carrier particle, (2) the partitioning rate of the drug out of the particle, and (3) the hydrolysis rate of the prodrug. In an ideal system, the particles should remain intact upon iv administration and be cleared relatively slowly from the central blood compartment. In addition, the prodrug should undergo rapid hydrolysis upon partitioning out of the delivery vehicle, preferably through enzymatic means rather than chemical hydrolysis to enhance stability in the formulation. The rate limiting process affecting drug availability is then the partitioning rate of the prodrug from the particle to the plasma compartment. A series of prodrugs based on paclitaxel as a model agent were investigated here in order to validate this general approach to achieving pharmacokinetic control in vivo.

Paclitaxel is a widely used chemotherapeutic agent for treating a range of carcinomas. The clinical material is formulated in a 50:50 mixture of ethanol and Cremophor EL (polyoxyethylenglyceroltriricinoleate) and is diluted with buffer prior to administration. There are many reports in the literature describing attempts to improve the formulation of paclitaxel using micelles, liposomes, or emulsions.⁷ In almost all cases, however, it is clear from the reported pharmacokinetic data that while these carriers formulate paclitaxel, they do not act as true delivery vehicles in vivo because the drug rapidly partitions out of the carrier with half-lives on the order of minutes. One reported exception appears to be a formulation of paclitaxel in micelles comprising poly(ethylene glycol)-poly(β -(4'-phenylbutanyl)aspartate).⁸

* To whom correspondence should be addressed. Phone: (604) 675-2120. Fax: (604) 708-5883. E-mail: sansell@celatorpharma.com.

[†] Celator Pharmaceuticals Corp.

[‡] Princeton University.

Many attempts have been made to produce functional lipophilic paclitaxel prodrugs to improve the performance of paclitaxel or to address formulations issues associated with the drug. These include conjugates with phospholipids,^{9,10} cholesterol,¹¹ α -bromo fatty acids,^{12,13} oleic acid,^{14,15} fullerene,¹⁶ and docosahexanoic acid.¹⁷ These prodrugs were formulated in lipid vehicles, such as liposomes,^{9,13,16} oil emulsions,^{14,15} or micelles.^{11,12,17} Most of these reports claim improved efficacy over paclitaxel in preclinical models; however, in most cases they either provide no information on plasma drug elimination or present data focusing on the terminal drug elimination phase rather than the early distribution phase. Drug elimination information during the first 24 h after administration is the period of most significant interest from a tumor delivery perspective because of the enhanced permeability and retention (EPR) phenomenon observed with particulate carriers, including micelles and nanoparticles.^{18–21}

In this work, the development of a series of lipophilic paclitaxel prodrugs and associated micellar/nanoparticle formulations is reported. Particulate delivery vehicles with prolonged circulation half-lives are described where the release of drug is modulated by manipulating the degree of lipid anchor hydrophobicity and the lability of the prodrug cross-linkers. The efficacy of the prodrugs in vivo is shown to be dependent on the nature of the linkage and the relative partitioning rate of the lipid anchor.

Results

Prodrug Synthesis. The prodrugs used in this study were based on the generalized structure paclitaxel–linker–lipid. The lipid anchors used were lipophilic alcohols, and these anchors were conjugated to paclitaxel using di-acid cross-linkers. This approach allowed both the anchor and the cross-linker to be varied independently in order to investigate the effects of changes in hydrolysis rates and partitioning behavior on the pharmacokinetics and efficacy for nanoparticle formulations of these prodrugs.

A range of commonly available lipid alcohols were used as the anchor component (Scheme 1), including α -tocopherol (**1** and **3**), oleyl alcohol (**2** and **4**), octadecanol (**5**), cosanol (**6**), docosanol (**7**), cholesterol (**8**), and 1,2-dimyristoyl-*sn*-glycerol (**9**). The lipids were conjugated to the cross-linker by treatment with the corresponding cyclic anhydride, followed by condensation of the anchor–linker product with paclitaxel using diisopropylcarbodiimide (DIPC) in the presence of *N,N*-4-dimethylaminopyridine (DMAP). Succinic acid (**1**, **2**) and diglycolic acid (**3**–**9**) were used as the cross-linkers. The 3-oxa moiety of the latter was intended to increase the susceptibility of the 2'-acyl group of the cross-linker to hydrolysis relative to the succinate analogues.

The 2'-acyl paclitaxel derivatives were prepared selectively by exploiting the difference in reaction rates between the paclitaxel 2'- and 7-hydroxyl groups.²² Under the reaction conditions used here, the majority of paclitaxel was consumed before significant levels of the 2',7-diacyl product were generated, as monitored by TLC. Column chromatography was used to remove unreacted paclitaxel, the 2',7-diacyl product, and other impurities in the crude reaction mixture. Purity and identity of the final products were confirmed by HPLC and NMR analysis, respectively.

Nanoparticle Formulation. The prodrugs were formulated in lipid-based nanoparticles by flash precipitation using a

confined volume impinging jet (CVIJ^a) mixer. This method involved rapid mixing of water and a miscible solvent containing the formulation components in a confined space using carefully controlled flow rates. Under conditions where the rate of mixing exceeds the rate of precipitation, these devices have been shown to achieve homogeneous particle formation kinetics, resulting in minimum sized particles for a particular formulation composition.^{23,24}

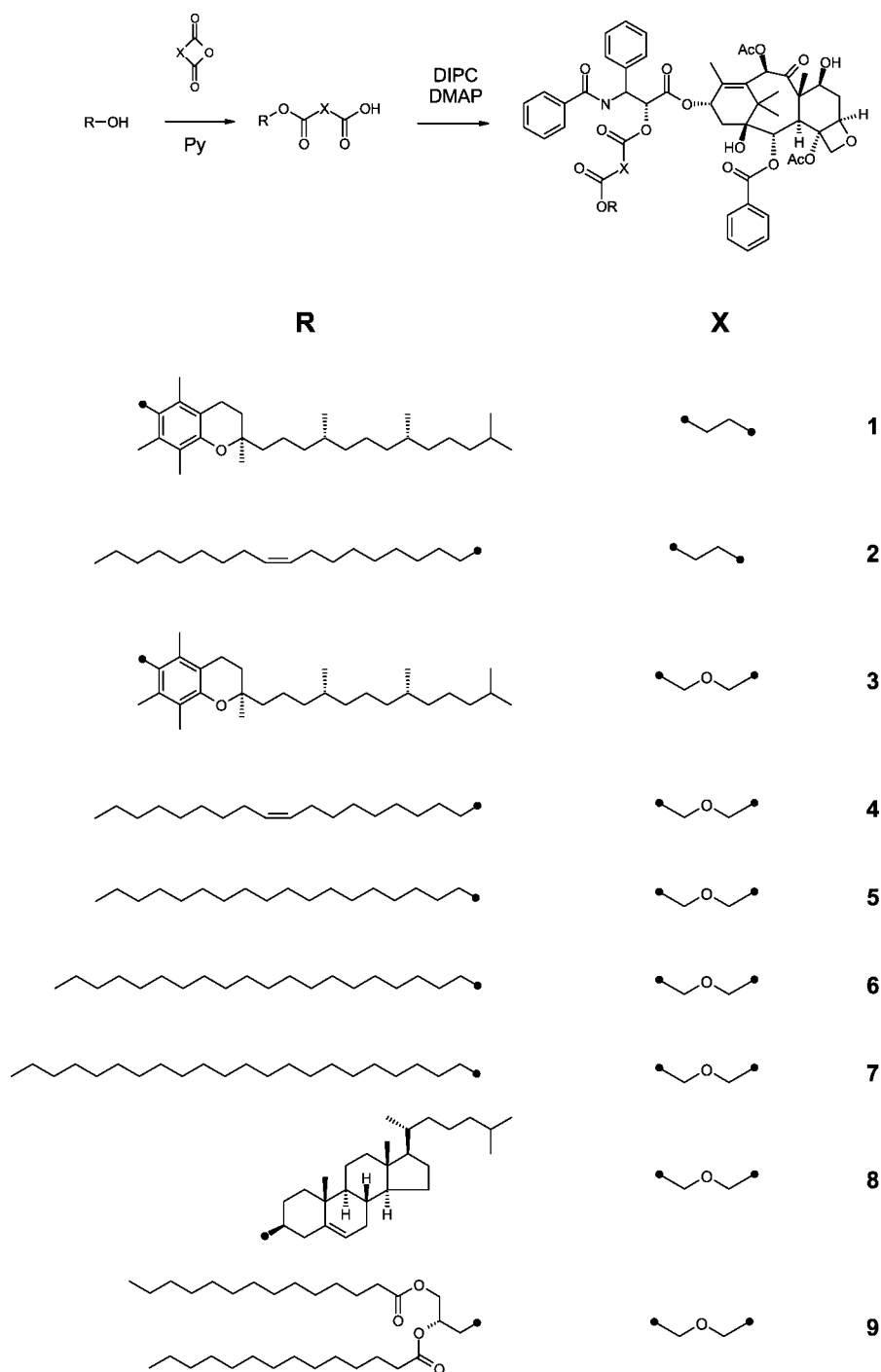
Formulations were composed of a prodrug, a co-lipid, and an amphipathic stabilizer in a weight ratio of 1:1:2 at a concentration of 40 mg per mL of solvent. The use of higher initial concentrations (>40 mg/mL) often led to the generation of large particles that compromised downstream handling of the preparation. The co-lipids used in this study were either α -tocopherol succinate (VES) or POPC, which facilitated processing. VES was replaced by POPC in later formulations because VES precipitated on long-term storage at 4 °C. Poly(ethylene glycol)-*b*-polystyrene (2kPS3k or 2.5kPS3k) was used as the amphipathic stabilizer. The application of a number of other stabilizers has been examined in formulations of this type and will be reported elsewhere. By use of the flash precipitation procedure, the mean particle diameter ranged from 10 to 20 nm for the prodrug/VES/2kPS3k nanoparticles and from 20 to 30 nm for the prodrug/POPC/2kPS3k nanoparticles.

Chemical and Physical Stability of Nanoparticle Formulations. The stability of nanoparticle formulations was monitored by HPLC after long-term storage at 4 °C. Analysis of **4**–**6** formulated with POPC/2kPS3k (1:1:2) in unbuffered 300 mM sucrose showed less than 5% free paclitaxel present after 11 weeks of storage. Free drug at that level was shown to have no antitumor activity in control efficacy experiments (data not shown). Accordingly, stability was considered adequate for the in vivo experiments carried out in these investigations.

Nanoparticle formulations stored in either sucrose solution or water at 4 °C were found to be physically stable for 3 months by visual inspection, with the exception of **8** which formed precipitates in some formulation compositions after 1–2 weeks of storage. Formulations using VES as the colipid also led to the slow formation of colloidal or crystalline precipitates, likely due to VES partitioning to the aqueous phase followed by subsequent precipitation outside the nanoparticle. VES formulations were therefore only suitable for short-term studies and not for longer term experiments such as efficacy evaluations.

The physical stability of formulations was investigated by examining changes in particle size after vortexing prodrug/co-lipid/2.5kPS3k (1:1:2) nanoparticles in water, 150 mM saline, or 300 mM sucrose (Table 1). These formulations consisted primarily of nanoparticles with diameters between 20 and 30 nm. Particles that were sensitive to mechanical stress underwent aggregation or phase separation when subjected to these conditions, resulting in the formation of larger particles in the sample. The increase in particle size was monitored by using dynamic light scattering to measure the Z average (the intensity weighted mean size of the particle distribution) value for samples before and after vigorous vortexing. The change in the Z_{ave} value was used as surrogate readout for the formation of aggregates or precipitates resulting from mechanical instability, where a higher value for ΔZ_{ave} indicated a higher level of aggregation

^a Abbreviations: VES, vitamin E succinate; POPC, 1-palmitoyl-2-oleoyl-*sn*-glycero-3-phosphocholine; CVIJ, confined volume impinging jets; 2kPS3k, poly(ethylene glycol)₂₀₀₀-*b*-polystyrene₃₀₀₀; 2.5kPS3k, poly(ethylene glycol)₂₅₀₀-*b*-polystyrene₃₀₀₀; ³H-CHE, tritiated cholesterol hexadecyl ether; TLC, thin layer chromatography; DIPC, diisopropylcarbodiimide; DMAP, *N,N*-4-dimethylaminopyridine.

Scheme 1. Synthesis of Lipophilic Paclitaxel Prodrugs

or precipitation (Table 1). Nanoparticles with POPC as the co-lipid were found to be significantly more stable in the presence of salt than those prepared with VES or in the absence of a co-lipid ($\Delta Z_{ave} = 24, 372$, and 774 nm, respectively, for formulations of **5**). In most cases mechanical stability was significantly improved in the presence of 300 mM sucrose compared to water. Sucrose samples where ΔZ_{ave} was in the range 0 – 40 nm had very little or no micrometer-sized material ($<2\%$ of the sample). Some prodrug formulations (**3** and **9**) that generated higher levels of aggregation in water and saline under these conditions ($\Delta Z_{ave} = 100$ – 200 nm) were stable in sucrose ($\Delta Z_{ave} = 0$ – 40 nm). The conclusion of the study was that the best stability was obtained using POPC co-lipids in nanoparticles formulated in 300 mM sucrose.

Similar results were obtained when samples were subjected to normal processing steps required for large sample preparations. Nanoparticles formulated in water or with either VES or no co-lipid were not stable when exposed to mechanical stress and exhibited significant precipitate formation during concentration steps using diafiltration. Stability while concentrating formulations could be improved by diluting the nanoparticle solution with sucrose for a final concentration of 300 mM prior to concentration. Use of POPC as the co-lipid provided further improvement of physical stability during storage and postformation processing, consistent with the results of the earlier stability studies. All of the concentrated samples used in this work subsequently were based on POPC as a co-lipid and were

Table 1. Physical Stability of Prodrug Formulations^a

prodrug	co-lipid	diameter (nm)	ΔZ_{ave} (nm)		
			water	150 mM saline	300 mM sucrose
2	POPC	26	20	43	10
3	POPC	24	125	55	42
4	POPC	22	15	25	5
5	POPC	21	20	24	7
6	POPC	23	21	26	36
7	POPC	23	18	24	0
8	POPC	23	47	42	41
9	POPC	23	167	171	0
5	VES	7	3	372	10
5		28	109	774	71

^a All formulations were prepared as prodrug/co-lipid/2.5kPS3k (1:1:2) nanoparticles in water. Particle diameter is the volume weighted average as determined with a Malvern Nano-ZS particle sizer. Stability was assessed by measuring the change in the Z_{ave} (ΔZ_{ave}) of samples diluted with equivolumes of water, 300 mM saline, or 600 mM sucrose after vortexing for 30 s.

prepared in 300 mM sucrose. Under these conditions precipitate formation was negligible up to drug concentrations of 8 mg/mL.

The diglycolate linkage was found to be more susceptible to hydrolysis over the succinate linkage, as may be predicted on the basis of the relative lability of the ester linkages. The increased reactivity of the diglycolate linkage posed an additional difficulty for accurate analysis of prodrug in biological samples. Methanol/acetonitrile 1:4 (v/v) was effective in near-complete precipitation of plasma proteins and liberation of the prodrug from the nanoparticle. However, a steady increase of free paclitaxel over time was observed after processing plasma samples, indicating hydrolysis during matrix workup and HPLC analysis. The diglycolate prodrug **6** was completely hydrolyzed after 9 h, while the succinate prodrug **2** was reduced to approximately 25% after 68 h. Hydrolysis was not observed when the samples were buffered with acetate at pH 4. Unbuffered samples of **6**/POPC/2kPS3k in the absence of plasma did not exhibit this hydrolysis, indicating that the time-dependent hydrolysis of prodrug in these formulations was most likely due to the presence of a nonprecipitated plasma component. This result suggests that the prodrug is stable when it is in the particle and that hydrolysis in biological media takes place after release of the prodrug.

In Vitro Activity. Evaluation of prodrug cytotoxicity was carried out using A2780 ovarian and MCF-7 breast human tumor cells treated with prodrug/POPC/2.5kPS3k (1:1:2) formulations prepared in distilled water (Table 2). Control formulations containing no prodrug confirmed that other nanoparticle components did not contribute to the growth inhibition of the cells. In addition, **1** was evaluated using a number of different nanoparticle formulations (**1**/VES/2kPS3k, **1**/2kPS3k, and **1**/cremophor) to show that the observed activity was independent of the type of formulation used.

Succinate-linked prodrugs (**1** and **2**) were found to be approximately 30- to 100-fold less potent than free paclitaxel against A2780 and MCF-7 cells. The decrease in observed activity was likely the result of resistance of the succinate group to hydrolysis. Subsequent prodrugs (**3–9**) were prepared with the diglycolate linker moiety, which was expected to be more susceptible to hydrolysis because of the presence of the 3-oxa group. The diglycolate prodrugs all showed similar potency in growth inhibition assays (50% growth inhibition concentration values, IC_{50} , of ~20 nM) and were an order of magnitude less potent than paclitaxel positive controls. The succinate analogues were always less potent than the corresponding diglycolate

Table 2. Inhibition of Human Tumor Cell Lines Using Prodrug/POPC/2kPS3k (1:1:2) Formulations^a

compd	$IC_{50} \pm SD$ (nM)	
	A2780	MCF-7
paclitaxel	2.4 \pm 0.3	3.8 \pm 0.6
1	192 \pm 18	158 \pm 72
2	75.1 \pm 3.9	67.0 \pm 5.9
3	25.3 \pm 1.3	13.4 \pm 2.4
4	28.4 \pm 1.4	15.9 \pm 0.7
5	20.9 \pm 10.9	15.1 \pm 1.5
6	29.0 \pm 1.3	16.6 \pm 4.5
7	29.5 \pm 5.2	23.5 \pm 1.3
8	27.0 \pm 1.1	24.1 \pm 0.6
9	34.7 \pm 1.3	32.2 \pm 1.3

^a The ovarian A2780 and breast MCF-7 human cell lines were evaluated for viability 72 h after drug addition using an MTT assay as outlined in the Experimental Section. IC_{50} values were determined for each of the three replicate studies with standard deviations (SD) presented.

prodrugs. For example, in the A2780 cell line the IC_{50} values for the succinate prodrug **1** and diglycolate prodrug **3** were 192 and 25.3 nM, respectively, compared to 2.4 nM for paclitaxel. Likewise, the succinate **2** and diglycolate **4** had IC_{50} values of 75.1 and 28.4 nM, respectively. These results are consistent with literature reports of related compounds, where IC_{50} values in the MCF-7 breast carcinoma cell line for paclitaxel, 2'-O-hexadecanoylpaclitaxel, and 2'-(2''-bromohexadecanoyl)paclitaxel were reported as <1, 8600, and 70 nM, respectively.¹³

In Vivo Nanoparticle Plasma Elimination. Partitioning rates for lipophilic drugs from lipid based particle formulations are commonly determined by dialysis of the drug carrier system against a bulk aqueous phase. The low aqueous solubility of the drug under these circumstances results in a high probability of the drug partitioning back into the carrier system rather than eluting through the dialysis membrane, resulting in artificially low apparent partitioning rates. Such an experiment does not accurately reflect behavior observed for hydrophobic drugs in vivo, where free drug can rapidly partition into the large hydrophobic reservoir present (for example, cell membranes or lipophilic proteins) rather than back into the delivery vehicle.⁵ Dialysis experiments therefore misrepresent the true delivery capability of these formulations. The most accurate means of determining true partitioning rates in vivo is to track both the drug and the particle using a nonexchangeable marker. Consequently it was necessary to identify such a marker and to confirm that it reflected the particle pharmacokinetics.

Elimination studies tracking both the prodrug and the particle were conducted to obtain a more accurate description of the partitioning behavior of the prodrugs in vivo (Figure 1). Prodrug elimination was followed by HPLC, while particle elimination rates were determined by labeling nanoparticles with tritiated cholesterylhexadecyl ether (³H-CHE). This label is widely used to track liposomes in vivo because it is regarded as a nonexchangeable, nonmetabolizable lipid marker in those systems. It was expected that the hydrophobicity and low level of hydration of this molecule would result in low partitioning rates from the nanoparticles used in this study and therefore would provide an assessment of particle fate, provided that particle integrity was maintained.

A number of experiments were carried out to determine the validity of the above assumptions and to approximate the particle plasma elimination rate. Formulations comprising **1**/VES/2kPS3k (1:1:2) and **2**/VES/2kPS3k (1:1:2) were labeled with trace amounts of ³H-CHE, and plasma levels of both the label and prodrug were monitored in Foxn1^{nu} mice (Figure 1A). The ³H-CHE label cleared at the same rate in both groups, with a

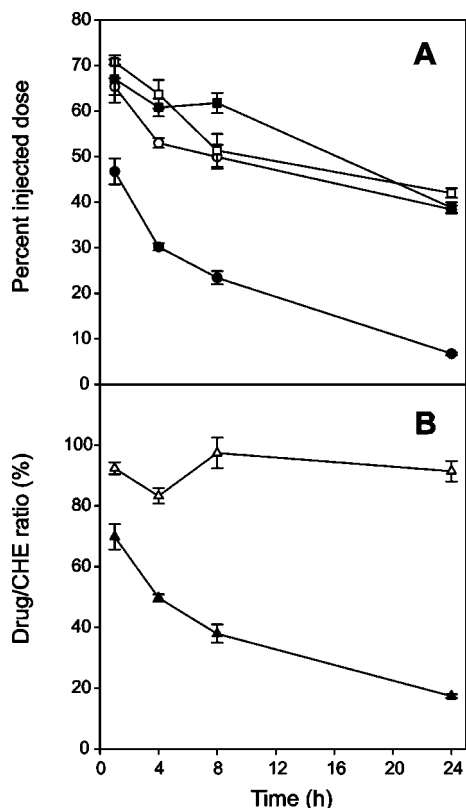


Figure 1. (A) Elimination of **1** (○) and **2** (●) in prodrug/VES/2kPS3k (1:1:2; w/w) formulations labeled with ^3H -CHE (□ and ■, respectively) in athymic nude Foxn1^{nu} mice dosed at 35 mg drug/kg doses ($n = 3/\text{time point}$). Drug concentrations were determined by HPLC analysis of plasma recovered at various time points. (B) Relative drug retention was determined using the ratio of drug/ ^3H -CHE in individual mice for **1** and **2** systems (ρ and π , respectively). Error bars represent standard deviation ($n = 3$).

half-life of approximately 24 h. Prodrug **1** cleared at approximately the same rate as ^3H -CHE in this system, while **2** was eliminated significantly faster. Comparison of prodrug/ ^3H -CHE ratios (Figure 1B) demonstrated that the ratio of **1** to particle label was virtually unchanged over the course of the experiment, suggesting that the partitioning half-life was significantly longer than the duration of the experiment. Prodrug **2** decreased relative to ^3H -CHE at a rate consistent with a partitioning half-life of approximately 4 h. The data in the experiment could be fitted to a four-parameter double-exponential decay implying that the partitioning rate constant changed over time, presumably in response to local environmental changes as drug partitioned out of individual particles.

The effects of formulation composition on elimination were determined by comparing the plasma elimination of **1** and ^3H CHE using 1/2kPS3k, 1/POPC/2kPS3k, and ^3H -CHE labeled 1/VES/2kPS3k (1:1:2) formulations in vivo (data not shown). For all three formulations both the label and prodrug elimination rates were found to be similar to that observed for **1** in Figure 1, indicating little to no role of co-lipid on the rate of elimination of **1** in these formulations. Additional elimination studies were performed using ^3H -CHE labeled 2kPS3k micelles and POPC/2kPS3k (1:2) nanoparticles, neither of which contained prodrug (data not shown). In both cases the ^3H -CHE label was cleared at approximately the same rate as observed for **1** in Figure 1. Finally, studies using 1/VES/3kPS3k and 1/VES/2.5kPS1.6k formulations demonstrated that moderate variations in the

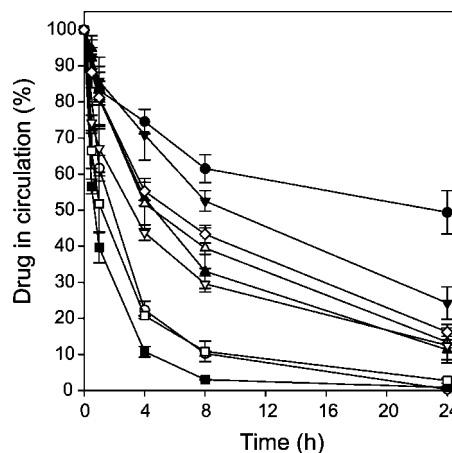


Figure 2. Elimination of prodrug formulated as prodrug/POPC/2kPS3k (1:1:2; w/w) formulations and administered intravenously to athymic nude Foxn1^{nu} mice at a dose of 7 mg/kg ($n = 3/\text{time point}$). Drug concentrations were determined by HPLC analysis of plasma isolated at various time points. The prodrugs used were **1** (●), **2** (○), **3** (◇), **4** (■), **5** (□), **6** (▲), **7** (△), **8** (▼), and **9** (▽). Error bars represent standard deviation ($n = 3$).

stabilizer poly(ethylene glycol)/polystyrene ratio had little effect on the elimination of **1** relative to that seen in Figure 1 (data not shown).

Elimination of **1** in these formulations was found to be independent of co-lipid and stabilizer composition and corresponded to the loss of the ^3H -CHE marker over time. These results suggest that the ^3H -CHE label remains with the particle throughout the pharmacokinetic experiment, independent of changes in the composition of the particle. The circulation half-lives for these particles were notably long (approximately 24 h), an order of magnitude longer than has been reported for micelles prepared using other polymers at these concentrations²⁵ and comparable to that observed with long-circulating liposomes.²⁶

Effect of Prodrug Partitioning on Plasma Drug Elimination. The prodrug panel was screened using prodrug/POPC/2kPS3k (1:1:2) nanoparticles in Foxn1^{nu} mice to determine elimination rates for the different prodrug conjugates (Figure 2). Prodrug circulation levels appeared to be dependent primarily on the prodrug partitioning rate and consequently indirectly reflect that rate, since the particles are sufficiently stable to remain intact over the course of the experiment. Conjugates were formulated at a concentration of 0.7 mg/mL. Variations in concentration did not appear to affect the particle elimination rate, since the relative rates of plasma elimination of 1/VES/2.5kPS1.6k (1:1:2) were independent of dose over the range 3–25 mg/kg (data not shown).

In order to estimate the partitioning half-life for each prodrug, it was assumed that **1** tracked the particle elimination rate based on the results discussed above. The elimination of all other prodrugs was then fitted to four-parameter double-exponential decay curves and normalized against **1**. The presence or absence of prodrug in the formulation did not significantly affect the elimination behavior of the particles, implying that changes in composition over time as drug partitioned out did not affect particle elimination rates. Prodrug elimination normalized to **1** therefore yielded a reasonable approximation of the relative partitioning half-lives of the prodrugs in these formulations.

Prodrug **1** had a negligible partitioning rate over 24 h, whereas **2** in this composition partitioned out with a half-life of approximately 1.7 h. Both of these prodrugs used succinate cross-linkers and were significantly less active than paclitaxel

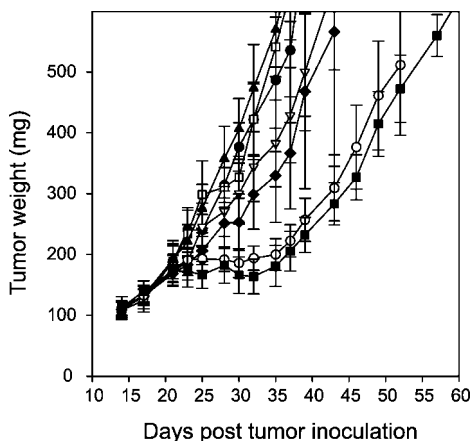


Figure 3. Relative efficacy of prodrugs formulated as prodrug/POPC/2kPS3k (1:1:2; w/w) nanoparticles when administered to athymic nude mice bearing HT29 human colon carcinoma xenographs. Drug was administered at a dose of $36 \mu\text{mol/kg}$ using a Q4D \times 6 schedule beginning on day 14. The prodrugs and controls used were saline (\bullet), 1 (\square), 2 (\blacktriangle), 4 (∇), 5 (\blacklozenge), 6 (\circ), 7 (\blacksquare). Error bars represent standard error of the mean ($n = 6$).

in vitro. The diglycolate versions of these compounds (**3** and **4**) showed accelerated elimination relative to their succinate parents, with partitioning half-lives of approximately 13 and 1 h, respectively. This is consistent with an increased level of hydration on partitioning into the aqueous phase due to the presence of the 3-oxa group of the diglycolate linkage.

The effect of small changes on the size of the lipid anchor was determined using the series **4**, **5**, **6**, and **7**, which have oleyl (ΔC18), stearyl (C18), cosanyl (C20), and docosanyl (C22) moieties, respectively. On the basis of the results in Figure 2, we estimated the partitioning half-lives for these prodrugs to be approximately 1, 1.7, 6.5, and 10 h, respectively. These results indicate that prodrug release from the nanoparticles can be regulated by adjusting the length of the alkyl anchor used.

The effect of other common lipid types on partitioning kinetics was also examined. A cholesteryl diglycolate conjugate (**8**) was retained considerably longer than the straight chain aliphatic species, with an estimated partitioning half-life of approximately 21 h. Unfortunately **8** was susceptible to phase separation from nanoparticles on storage and was not fully evaluated in later efficacy studies in this work. A 1,2-dimyristoyl-*sn*-glycero-3-succinate derivative (**9**) was evaluated in anticipation that it would be better retained than **7** since it had two C14 anchors; however, it partitioned out more quickly, with a half-life of 8.5 h. The higher partitioning rate was likely due to increased levels of hydration on the glycerol backbone during exchange out of the nanoparticle.

Efficacy of Paclitaxel Prodrug Conjugates in Nanoparticle Formulations. The relative efficacies of nanoparticle formulations of **1**–**7** were determined in the HT29 human colorectal xenograft solid tumor model using a $36 \mu\text{mol/kg}$ dose on a Q4D \times 6 schedule (Figure 3). Saline was used as a negative control. Earlier experiments conducted with submaximal doses suggested that this dose would result in a range of responses bracketing the behaviors of positive and negative control groups and in this way would allow discernment of the relative therapeutic potencies of the individual prodrug species. Prodrug **8** was not included in the study because of precipitation of drug from formulations on storage. Prodrugs **3** and **9** were omitted as well because their partitioning half-lives were similar to those of **6** and **7**.

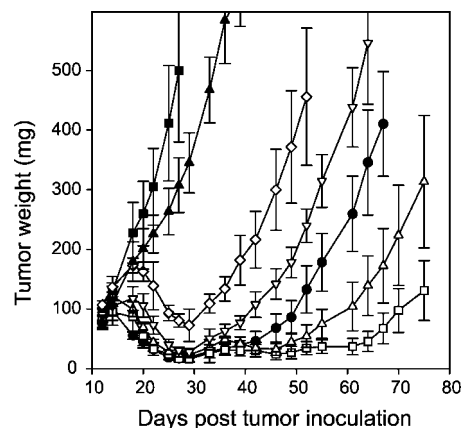


Figure 4. Effect of dose on the efficacy of 7/POPC/2kPS3k nanoparticles in the HT29 human colon carcinoma model. Athymic nude mice were injected intravenously with formulations 14 days after tumor cell inoculation. 7/POPC/2kPS3k (1:1:2) was administered at $69 \mu\text{mol/kg}$ (3 paclitaxel equiv, \square), $46 \mu\text{mol/kg}$ (2 paclitaxel equiv, Δ), $34 \mu\text{mol/kg}$ (1.5 paclitaxel equiv, ∇), $23 \mu\text{mol/kg}$ (1 paclitaxel equiv, \diamond), and $5.7 \mu\text{mol/kg}$ (0.25 paclitaxel equiv, \blacktriangledown) using a Q2D \times 5 schedule. Saline (Q2D \times 5, \bullet) was used as a negative control. Paclitaxel was administered at $23 \mu\text{mol/kg}$ using a Q2D \times 5 (\bullet) dosing schedule. Error bars represent standard error of the mean ($n = 6$). All treatments were initiated on day 12 after tumor cell inoculation.

The two succinate linked prodrugs, **1** and **2**, showed no evidence of any therapeutic activity at the $34 \mu\text{mol/kg}$ dose. The results correlated with the observation that these prodrugs were 2 orders of magnitude less potent than paclitaxel in in vitro cell growth inhibition assays (Table 2). The partitioning half-lives of **2** and **1** differed widely, ranging from 1.7 h with **2** to effectively nonexchangeable on experimental time frames with **1**. These results indicate that even though the succinate-linked species **2** is being made available to cells, the lower hydrolysis rate and concomitant release of paclitaxel are insufficient to provide a meaningful therapeutic response.

The four diglycolate linked species, **4**–**7**, all resulted in varying degrees of inhibition of tumor growth. In vitro growth inhibition studies of these prodrugs had demonstrated that the cytotoxicity of diglycolate-linked prodrugs was greater than their succinate analogues (Table 2). Elimination data for these formulations indicated that aliphatic chain length was related to partitioning half-lives for the prodrugs, which were 1, 1.7, 6.5, and 10 h, respectively. This correlates well with the observed efficacy trends, where the greatest antitumor response is seen with the prodrug having the longest partitioning half-life, namely, the docosanyl conjugate **7**. Relative efficacy was determined using the treatment induced delay in reaching a mean tumor size of 500 mm^3 , yielding values of 3, 4, 15, and 17 days, respectively. On the basis of these results, further investigations to optimize dose and scheduling using the nanoparticle formulation of **7** were undertaken.

Effect of Dose on the Efficacy of 7. The activity of **7** in POPC/2.5kPS3k nanoparticle formulations relative to paclitaxel was determined by comparing the efficacy of doses ranging from 0.25 to 3 mol equiv of paclitaxel (Figure 4) in the HT29 tumor model. The Q2D dosing regime was chosen because the greatest efficacy for **7** and paclitaxel was observed on this schedule. Sporadic deaths were observed with paclitaxel during the sixth dose when administered at 20 mg/kg ($23 \mu\text{mol/kg}$), consistent with reported literature values.^{12,17,27} The Q2D \times 5 schedule was chosen for the study to avoid this apparent Cremophor related toxicity. The maximum tolerated dose of **7** on the Q2D \times 5 schedule was approximately 3 paclitaxel equiv ($69 \mu\text{mol/kg}$).

Dosing at 4 paclitaxel equiv (92 $\mu\text{mol/kg}$) resulted in weight loss in excess of 15% over the course of treatment.

The tumor growth data were analyzed by two methods to determine what dose of **7** would be equivalent to the paclitaxel positive control. In the first method only the treatment groups that resulted in tumor regression were considered. The delay in reaching a tumor size of 125 mg was measured from the start of treatment and then normalized against the delay observed for the paclitaxel group. The relative delay was plotted against paclitaxel dose equivalents of **7**, yielding a data set that showed a linear dose response up to the MTD of **7**. The fitted curve indicated that **7** achieved parity with paclitaxel at a dose of 1.75 dose equiv of paclitaxel. In the second analysis the delay in reaching a tumor size of 300 mg was measured relative the saline negative control and then normalized against the delay observed for the paclitaxel group. Plotting the relative delay against paclitaxel dose equivalents of **7** again yielded a linear dose response that showed that parity with the paclitaxel group was achieved with 1.65 paclitaxel equiv of **7**. Importantly, when the nanoparticle formulation of **7** was dosed at 3 molar paclitaxel equiv (69 $\mu\text{mol/kg}$), reflecting its MTD, the antitumor activity was significantly greater than that achieved with Cremophor formulated paclitaxel administered at its MTD. Specifically, tumors treated with the nanoparticle formulation of **7** at MTD remained below 50 mg at day 60 in contrast to tumors treated with paclitaxel at MTD, which had grown to nearly 300 mg (Figure 4).

Discussion

The nanoparticle delivery system employed in this work required the synthesis of paclitaxel prodrugs to increase the hydrophobicity of the drug. While paclitaxel itself is nearly insoluble in water, it possesses sufficient aqueous solubility that it can rapidly partition out of lipid-based delivery systems, typically with half-lives on the order of a few minutes.^{28–30} The objective of this work was to control the pharmacokinetics of the formulated drug in vivo while maximizing efficacy. A variety of prodrugs were synthesized, characterized, and formulated into nanoparticles to characterize the effects of iterative changes to the anchor–linker–drug structural motif on partition kinetics and efficacy. A spectrum of in vitro and in vivo antitumor activity was observed, dictated by the physical and chemical properties of the prodrug rather than the delivery vehicle itself.

Nanoparticle formulations of the type reported here are most likely cleared as a result of single polymer chains partitioning out of the particle over time in vivo. Gradual loss of the stabilizer component destabilizes the particle and would result in the elimination of any payload that had not already partitioned out. We expect that particles with a high drug/stabilizer ratio would be cleared rapidly because the loss of relatively small amounts of polymer exposes the particle core to potential protein interactions. Particles with low drug/stabilizer ratios have greater tolerance to loss of polymer and may survive long enough to be cleared through other mechanisms in vivo. This implies that an ideal delivery system should approach the size of a micelle with a relatively low drug/polymer ratio, preferably with a stabilizer that has a low partitioning rate.

Prodrugs with lipid anchors of different hydrophobicity demonstrated different partition rates from the same particle composition. In these nanoparticles, drug physicochemical properties largely dictated the release of drug from the carrier rather than degradation of the carrier itself. This behavior leads to a significant difference between paclitaxel in Cremophor and

paclitaxel prodrugs in nanoparticles. Paclitaxel partitions rapidly out of Cremophor micelles on injection and distributes broadly to lipophilic sinks it encounters in the blood compartment. Over time the drug redistributes back into the blood compartment before being cleared.^{29,30} Prodrug nanoparticles do not exhibit this early distribution phase but rather are continually releasing drug over time, the rate of which depends on the partitioning rate of the prodrug component. The prodrug partitioning rate was shown to be directly correlated to efficacy (Figures 2 and 3), and this rate was readily tunable by varying the lipid anchor (and hence hydrophobicity) of the prodrug.

The dependence of efficacy on partitioning rate can be rationalized in terms of accumulation of nanoparticles in tumors followed by gradual release of prodrug. Nanoparticles that release their payload rapidly or are cleared rapidly from circulation will deliver less drug to the tumor site and consequently may be expected to exhibit reduced efficacy. Preliminary in vivo particle distribution studies indicated that tumor accumulation levels plateau at $\sim 3\%$ of the injected dose per gram of tumor tissue, with the majority of the accumulation occurring within the first 8 h. Similar results have been reported in the literature.^{18–21} In the case of prodrugs such as **4** and **5** where partitioning half-lives are approximately 1 and 1.7 h, respectively, the level of drug delivered to tumors is expected to be significantly lower, likely accounting for the reduced efficacy observed for these species. Prodrugs **6** and **7** release drug at slower rates, with partitioning half-lives of approximately 6.5 and 10 h, respectively. Since the particle accumulation in tumor is expected to be similar in all cases, formulations with these prodrugs are capable of delivering more drug to the tumor.

The effects of dose on the efficacy of **7** nanoparticles were evaluated relative to commercially formulated paclitaxel. The optimal therapeutic response was observed with a Q2D dosing in the HT29 solid tumor model. The nanoparticles used to formulate **7** have an elimination half-life of approximately 24–36 h, while **7** itself has a partitioning half-life of about 10 h. These values are consistent with an effective release of prodrug at the tumor site over a period of approximately 2 days postadministration, coinciding with the Q2D schedule. Titration of drug dose through 0.25–3 paclitaxel equiv compared to paclitaxel at MTD showed that **7** achieved equivalent efficacy at approximately 1.7 paclitaxel equiv. Since the dose response for **7** is linear up to the MTD, it is possible to significantly improve efficacy over the maximum tolerated dose of paclitaxel using higher doses of **7**. We expect that prodrugs that are better retained than **7** in nanoparticles would achieve parity at lower doses than that seen for **7**, offering the potential for further improvement of this nanoparticle system.

A major driving force in the development of the prodrug nanoparticles described here is the generation of delivery systems in which two drugs are released at matched rates to maintain a synergistic ratio. The purpose of this study was to demonstrate that it is possible to control drug release using a paclitaxel as a model agent. Improved performance over the free drug in vivo could be achieved through adjustment of prodrug properties and complementary design of the delivery system. This technology provides a delivery platform from which synergistic combinations of different prodrug conjugates can be coformulated in nanoparticles that are able to maintain the desired drug/drug ratio in vivo, thereby optimizing synergy and avoiding antagonism.

Experimental Section

Materials. All reagents unless otherwise specified were purchased from Sigma-Aldrich Canada Ltd., Oakville, Ontario. Sol-

vents were obtained from VWR International, Mississauga, Ontario. Paclitaxel was purchased from Indena S.p.A., Milan, Italy. ^3H -CHE was obtained from Perkin-Elmer Life and Analytical Sciences, Inc., Waltham, MA. POPC was obtained from Northern Lipids, Burnaby, British Columbia. ^1H NMR spectra were recorded in CDCl_3 on a Bruker Avance 400. HT-29 human colorectal adenocarcinoma cells were obtained from ATCC, Manassas, VA. Foxn1tm mice were obtained from Harlan, Indianapolis, IN. The confined volume impinging jets mixer was custom-built at Princeton University. All animal experiments were conducted according to protocols approved by the University of British Columbia's Animal Care Committee and in accordance with the current guidelines established by the Canadian Council of Animal Care.

Synthesis of Lipid Anchors. A lipid alcohol in pyridine was treated with 3 equiv of succinic anhydride or diglycolic anhydride at room temperature overnight. The solvent was removed on a rotovap and the residue extracted from dilute hydrochloric acid with methylene chloride. The organic fractions were dried over anhydrous magnesium sulfate and filtered, and the solvent was removed. Conversion to the appropriate acid was monitored by TLC, which in most cases was 100%. The resultant product was either dried under vacuum or lyophilized from benzene. The lipid acids were used in the following steps without further purification.

Synthesis of Paclitaxel Conjugates. Paclitaxel (1 equiv), a lipid acid (2 equiv), and 4-*N,N*-dimethylaminopyridine (3 equiv) were dissolved in alcohol-free chloroform. Diisopropylcarbodiimide (1.3 equiv) was then added and the solution stirred at room temperature. The reaction was monitored by TLC until most of the paclitaxel had been consumed (typically 2–4 h). The reaction mixture was then washed with dilute hydrochloric acid and dried over anhydrous magnesium sulfate. After removal of solvent the crude product was passed down a silica gel column using a methanol/methylene chloride gradient. The purified prodrug was lyophilized from benzene and stored at room temperature.

2'-O-(4''-O-Tocopherylsuccinoyl)paclitaxel 1. **1** was synthesized from paclitaxel and tocopherol succinate. ^1H NMR (400 MHz, CDCl_3) δ 3.83 (1H, d, J = 7.25 Hz), 4.22 (1H, d, J = 8.60 Hz), 4.33 (1H, d, J = 8.60 Hz), 4.46 (1H, dd, J = 10.88 Hz, J' = 6.58 Hz), 4.99 (1H, d, J = 9.54 Hz), 5.52 (1H, d, J = 3.22 Hz), 5.70 (1H, d, J = 6.98 Hz), 5.98 (1H, dd, J = 9.13 Hz, J' = 3.22 Hz), 6.27 (1H, t, J = 8.6 Hz), 6.97 (1H, d, J = 8.87 Hz).

2'-O-(4''-O-Oleylsuccinoyl)paclitaxel 2. **2** was synthesized from paclitaxel and oleyl succinate. ^1H NMR (400 MHz, CDCl_3) δ 3.82 (1H, d, J = 7.0 Hz), 3.96 (2H, t, J = 6.81 Hz), 4.21 (1H, d, J = 8.38 Hz), 4.33 (1H, d, J = 8.38 Hz), 4.46 (1H, br. s), 4.98 (1H, d, J = 8.45 Hz), 5.36 (2H, m), 5.50 (1H, d, J = 2.89 Hz), 5.69 (1H, d, J = 7.00 Hz), 6.00 (1H, dd, J = 9.04 Hz, J' = 2.74 Hz), 6.26 (1H, t, J = 8.91 Hz), 7.08 (1H, d, J = 9.06 Hz).

2'-O-(5''-O-Tocopheryldiglycoloyl)paclitaxel 3. **3** was synthesized from paclitaxel and tocopherol diglycolate. ^1H NMR (400 MHz, CDCl_3) δ 3.84 (1H, d, J = 6.98 Hz), 4.22 (1H, d, J = 8.3 Hz), 4.34 (1H, d, J = 8.6 Hz), 4.99 (1H, d, J = 7.79 Hz), 5.64 (1H, d, J = 2.96 Hz), 5.70 (1H, d, J = 6.98 Hz), 6.06 (1H, dd, J = 9.27 Hz, J' = 2.82 Hz), 6.30 (1H, t), 6.97 (1H, d, J = 9.13 Hz).

2'-O-(5''-O-Oleyldiglycoloyl)paclitaxel 4. **4** was synthesized from paclitaxel and oleyl diglycolate. ^1H NMR (400 MHz, CDCl_3) δ 3.83 (1H, d, J = 7.0 Hz), 4.46 (1H, t, J = 7.96 Hz), 4.99 (1H, d, J = 8.45 Hz), 5.35 (2H, m), 5.60 (1H, d, J = 2.74 Hz), 5.70 (1H, d, J = 7.08 Hz), 6.05 (1H, dd, J = 9.25 Hz, J' = 2.55 Hz), 6.28 (1H, t, J = 8.9 Hz), 7.04 (1H, d, J = 9.29 Hz).

2'-O-(5''-O-Octadecyldiglycoloyl)paclitaxel 5. **5** was synthesized from paclitaxel and octadecyl diglycolate. ^1H NMR (400 MHz, CDCl_3) δ 3.83 (1H, d, J = 7.0 Hz), 4.46 (1H, dd, J = 10.74 Hz, J' = 6.70 Hz), 4.99 (1H, d, J = 8.45 Hz), 5.60 (1H, d, J = 2.82 Hz), 5.70 (1H, d, J = 7.00 Hz), 6.05 (1H, dd, J = 9.25 Hz, J' = 2.55 Hz), 6.28 (1H, t, J = 8.9 Hz), 7.05 (1H, d, J = 9.29 Hz).

2'-O-(5''-O-Cosanyldiglycoloyl)paclitaxel 6. **6** was synthesized from paclitaxel and cosanyl diglycolate. ^1H NMR (400 MHz, CDCl_3) δ 3.83 (1H, d, J = 6.98 Hz), 4.0–4.4 (5H, m), 4.46 (1H, dd, J = 10.75 Hz, J' = 6.72), 4.99 (1H, d, J = 9.40 Hz), 5.60 (1H,

d, J = 2.96 Hz), 5.70 (1H, d, J = 7.25 Hz), 6.05 (1H, dd, J = 9.27 Hz, J' = 2.82), 6.29 (1H, t, J = 8.3 Hz), 7.05 (1H, d, J = 9.13 Hz).

2'-O-(5''-O-Docosanyldiglycoloyl)paclitaxel 7. **7** was synthesized from paclitaxel and docosanyl diglycolate. ^1H NMR (400 MHz, CDCl_3) δ 3.83 (1H, d, J = 6.98 Hz), 4.0–4.4 (5H, m), 4.46 (1H, dd, J = 10.75 Hz, J' = 6.72 Hz), 4.99 (1H, dd, J = 9.40 Hz, J' = 1.61 Hz), 5.60 (1H, d, J = 2.96 Hz), 5.70 (1H, d, J = 6.98 Hz), 6.05 (1H, dd, J = 9.40 Hz, J' = 2.95 Hz), 6.28 (1H, t, J = 8.3 Hz), 7.05 (1H, d, J = 9.40 Hz).

2'-O-(5''-O-Cholesteryldiglycoloyl)paclitaxel 8. **8** was synthesized from paclitaxel and cholesteryl diglycolate. ^1H NMR (400 MHz, CDCl_3) δ 3.83 (1H, d, J = x Hz), 4.0–4.4 (5H, m), 4.47 (1H, dd, J = 10.6 Hz, J' = 6.8 Hz), 4.63 (1H, m), 4.99 (1H, d, J = 7.79 Hz), 5.38 (1H, d, J = 3.76 Hz), 5.61 (1H, d, J = 2.69 Hz), 5.70 (1H, d, J = 7.25 Hz), 6.06 (1H, dd, J = 9.13 Hz, J' = 2.69 Hz), 6.28 (1H, t, J = 8.3 Hz), 7.09 (1H, d, J = 9.40 Hz).

2'-O-(5''-O-(1''',2'''-Dimyristoyl-sn-glycero)diglycoloyl)paclitaxel 9. **9** was synthesized from paclitaxel and 3-(1,2-dimyristoyl-sn-glycerol) diglycolate. ^1H NMR (400 MHz, CDCl_3) δ 3.84 (1H, d, J = 6.98 Hz), 4.47 (1H, dd, J = 10.6 Hz, J' = 6.8 Hz), 4.99 (1H, dd, J = 9.54 Hz, J' = 1.75 Hz), 5.20 (1H, m), 5.61 (1H, d, J = 2.96 Hz), 5.71 (1H, d, J = 7.25 Hz), 6.07 (1H, d, J = 9.27 Hz, J' = 2.82 Hz), 6.31 (1H, t), 7.11 (1H, d, J = 9.40 Hz).

Nanoparticle Formulation. The prodrug, co-lipid, and stabilizer polymers (typically on a 1:1:2 w/w basis) were dissolved in ethanol/THF (4:1) at a concentration of 40 mg/mL. The solvent was rapidly diluted with water using a four-port CVII mixer^{23,24} with flow rates set at 12/12/53/53 mL/min (solvent/water/water/water). Flow rates were controlled using Harvard apparatus PHD2000 syringe pumps. The resultant solution was then dialyzed against water to remove residual solvent. The final drug concentration was typically about 0.7 mg/mL. When higher concentrations were required, the dialyzed solution was diluted with equivolumes of 600 mM sucrose and then concentrated using a 100 kD, 0.5 mm lumen, 60 cm path length MidGee hoop cartridge (GE Healthcare Life Sciences, Piscataway, NJ) with a peristaltic pump. Particle size was determined using a Malvern Zetasizer Nano-ZS particle sizer and reported as volume weighted data.

In Vitro Activity. The MCF-7 human tumor cell line was purchased from American Type Culture Collection (MEM media supplemented with 2 mM L-glutamine and 10% FBS). The A2780 human tumor cell line was purchased from the European Collection of Cell Culture (RPMI 1640 media supplemented with 2 mM L-glutamine and 10% FBS). Cultures were incubated at 37 °C and 5% CO_2 .

On day 0, A2780 cells were plated at 2000 cells/well and MCF-7 cells at 1500 cells/well and allowed to adhere for 24 h. On day 1 cells were exposed in triplicate to a 2-fold serial dilution of prodrug/POPC/2.5kPS3k (1:1:2) nanoparticle formulations for 72 h at 16 concentrations. Viable cells were quantified using standard 3-(4,5-dimethylthiazol-2-yl)-2,5-diphenyltetrazolium bromide (MTT) detection at 570 nm after DMSO addition.³¹ Survival rate after treatment is expressed as a mean percentage relative to untreated control wells.

In Vivo Plasma Elimination. Athymic nude mice (n = 3/time point) were injected iv with test samples (10 μL /g body weight, to a maximum of 250 μL). Blood was collected at the designated time point by cardiac puncture and placed into EDTA coated microtainer tubes (BD Biosciences). The tubes were centrifuged at 2800 rpm for 10 min. Plasma was recovered, and 50 μL aliquots were analyzed by HPLC for drug content. Samples containing ^3H -CHE (50 μL) were diluted with Picofluor40 scintillation fluid (Packard) and counted on a Beckman-Coulter LS 6500 multipurpose scintillation counter. The total drug (counts) per mouse in the blood compartment was calculated assuming a plasma volume of 0.041 25 mL per gram of body weight.

In Vivo Efficacy. Female athymic nude mice (7–8 weeks old) were inoculated subcutaneously with 100 μL of HT29 human colon carcinoma cells (2×10^6 cells) using a 26 gauge needle. Mice were randomly grouped (n = 6/group) with a mean tumor size between

80 and 120 mg prior to the first treatment. (Tumors greater than 200 mg and smaller than 30 mg were excluded.) Test samples were injected with a volume of 10 μ L drug/g body weight, to a maximum of 250 μ L. Subsequent injections were made according to the designated schedule. Tumor length and width measurements, body weight, and in life observations were recorded 2–3 times per week. Tumor weight was calculated according to the formula $(L)(W^2)/2$.

The paclitaxel positive controls were administered using the commercial clinical formulation Taxol. Taxol comprises a 6 mg/mL solution of paclitaxel dissolved in 527 mg of Cremophor EL/49.7% (v/v) ethanol and was reconstituted immediately prior to administration by dilution with 0.9% saline in a 1:2 ratio (v/v) for a final paclitaxel concentration of 2 mg/mL.

HPLC Analysis. Plasma samples (50 μ L) or nanoparticle suspensions (50 μ L) were mixed with 150 μ L of diluents (methanol/acetonitrile, 2:1 v/v) by vigorous vortexing followed by centrifugation at 10000g for 10 min. Supernatant (20 μ L) was injected into a Waters HPLC for quantitation using a Phenomenex SynergiFusion reverse phase analytical column monitored by UV detection at 227 nm. Chromatography was conducted with a 1 mL/min gradient elution of methanol and 10 mM sodium acetate buffer (pH 5.6) mobile phases from an initial solvent mix of 70:30 to 100:0, respectively. Column temperature was set at 30 °C. Samples were kept in the autosampler compartment at 4 °C prior to HPLC analysis.

Acknowledgment. We thank Suzen Lines, Lindsey Knight, Fiona Ross, and Sarah Kelly for assistance in the vivarium.

Supporting Information Available: NMR and HPLC data, elimination curves for control particles, modeled partition data, relative weight loss data for Figure 4. This material is available free of charge via the Internet at <http://pubs.acs.org>.

References

- (1) Harasym, T. O.; Tardi, P. G.; Harasym, N. L.; Harvie, P.; Johnstone, S. A.; Mayer, L. D. Increased preclinical efficacy of irinotecan and floxuridine coencapsulated inside liposomes is associated with tumor delivery of synergistic drug ratios. *Oncol. Res.* **2007**, *16*, 361–374.
- (2) Mayer, L. D.; Janoff, A. S. Optimizing combination chemotherapy by controlling drug ratios. *Mol. Interventions* **2007**, *7*, 216–223.
- (3) Harasym, T. O.; Tardi, P. G.; Johnstone, S. A.; Bally, M. B.; Janoff, A. S.; Mayer, L. D. Fixed Drug Ratio Liposome Formulations of Combination Cancer Therapeutics. In *Liposome Technology*, 3rd ed.; Gregoriadis, G. Ed.; Informa Healthcare: New York, 2007; Volume III, pp 25–48.
- (4) Mayer, L. D.; Harasym, T. O.; Tardi, P. G.; Harasym, N. L.; Shew, C. R.; Johnstone, S. A.; Ramsay, E. C.; Bally, M. B.; Janoff, A. S. Ratiometric dosing of anticancer drug combinations: controlling drug ratios after systemic administration regulates therapeutic activity in tumor-bearing mice. *Mol. Cancer Ther.* **2006**, *5*, 1854–1863.
- (5) Fahr, A.; van Hoogevest, P.; May, S.; Bergstrand, N.; Leigh, M. L. S. Transfer of lipophilic drugs between liposomal membranes and biological interfaces: consequences for drug delivery. *Eur. J. Pharm. Sci.* **2005**, *26*, 251–265.
- (6) Skwarczynski, M.; Hayashi, Y.; Kiso, Y. Paclitaxel prodrugs: toward smarter delivery of anticancer agents. *J. Med. Chem.* **2006**, *49*, 7253–7269.
- (7) Hennenfent, K. L.; Govindan, R. Novel formulations of taxanes: a review. Old wine in a new bottle. *Ann. Oncol.* **2006**, *17*, 734–749.
- (8) Hamaguchi, T.; Matsumura, Y.; Suzuki, M.; Shimizu, K.; Goda, R.; Nakamura, I.; Yokoyama, M.; Kataoka, K.; Kakizoe, T. NK105, a paclitaxel-incorporating micellar nanoparticle formulation, can extend in vivo antitumor activity and reduce the neurotoxicity of paclitaxel. *Br. J. Cancer* **2005**, *92*, 1240–1246.
- (9) Ansell, S. Lipophilic Drug Derivatives for Use in Liposomes. U.S. Patent 5,534,499, 1996.
- (10) Hostetler, K. Y.; Sridhar, N. C. Prodrugs for Oral Administration Containing Taxol Covalently Bound to a Phospholipid. U.S. Patent 5,484,809, 1996.
- (11) Stevens, P. J.; Sekido, M.; Lee, R. J. A folate receptor-targeted lipid nanoparticle formulation for a lipophilic paclitaxel prodrug. *Pharm. Res.* **2004**, *21*, 2153–2157.
- (12) Perkins, W. R.; Ahmad, I.; Li, X.; Hirsh, D. J.; Masters, G. R.; Fecko, C. J.; Lee, J. K.; Ali, S.; Nguyen, J.; Schupsky, J.; Herbert, C.; Janoff, A. S.; Mayhew, E. Novel therapeutic nano-particles lipocores: trapping poorly water soluble compounds. *Int. J. Pharm.* **2000**, *200*, 27–39.
- (13) Ali, S.; Ahmad, I.; Peters, A.; Masters, G.; Minchey, S.; Janoff, A. S.; Mayhew, E. Hydrolyzable hydrophobic taxanes: synthesis and anticancer activities. *Anti-Cancer Drugs* **2001**, *12*, 117–128.
- (14) Lundberg, B. B.; Risovic, V.; Ramaswamy, M.; Wasan, K. M. A lipophilic paclitaxel derivative incorporated in a lipid emulsion for parenteral administration. *J. Controlled Release* **2003**, *86*, 93–100.
- (15) Rodrigues, D. C.; Maria, D. A.; Fernandes, D. C.; Valduga, C. J.; Couto, R. D.; Ibanez, O. C. M.; Maranhao, R. C. Improvement of paclitaxel therapeutic index by derivatization and association to a cholesterol-rich microemulsion: in vitro and in vivo studies. *Cancer Chemother. Pharmacol.* **2005**, *55*, 565–576.
- (16) Zakharian, T. Y.; Seryshev, A.; Sitharaman, B.; Gilbert, B. E.; Knight, V.; Wilson, L. J. A fullerene-paclitaxel chemotherapeutic: synthesis, characterization and study of biological activity in tissue culture. *J. Am. Chem. Soc.* **2005**, *127*, 12508–12509.
- (17) Bradley, M. O.; Webb, N. L.; Anthony, F. H.; Devanesan, P.; Witman, P. A.; Hemamalini, S.; Chander, M. C.; Baker, S. D.; He, L.; Horwits, S. B.; Swindell, C. S. Tumor targeting by covalent conjugation of a natural fatty acid to paclitaxel. *Clin. Cancer Res.* **2001**, *7*, 3229–3238.
- (18) Torchilin, V. P. Lipid-core micelles for targeted drug delivery. *Curr. Drug Delivery* **2005**, *2*, 319–327.
- (19) Kwon, G.; Suwa, S.; Yokoyama, M.; Okano, T.; Sakurai, Y.; Kataoka, K. Enhanced tumor accumulation and prolonged circulation times of micelle-forming poly (ethylene oxide-aspartate) block copolymer-adriamycin conjugates. *J. Controlled Release* **1994**, *29*, 17–23.
- (20) Weissig, V.; Whiteman, K. R.; Torchilin, V. P. Accumulation of protein-loaded long-circulating micelles and liposomes in subcutaneous Lewis lung carcinoma in mice. *Pharm. Res.* **1998**, *15*, 1552–1556.
- (21) Lukyanov, A. N.; Gao, Z.; Mazzola, L.; Torchilin, V. P. Polyethylene glycol–diacyllipid micelles demonstrate increased accumulation in subcutaneous tumors in mice. *Pharm. Res.* **2002**, *19*, 1424–1429.
- (22) Deutsch, H. M.; Glinski, J. A.; Hernandez, M.; Haugwitz, R. D.; Narayanan, V. L.; Suffness, M.; Zalkow, L. H. Synthesis of congeners and prodrugs. 3. Water-soluble prodrugs of Taxol with potent antitumor activity. *J. Med. Chem.* **1989**, *32*, 788–792.
- (23) Johnson, B. K.; Prud'homme, R. K. Flash nanoprecipitation of organic actives and block copolymers using a confined impinging jets mixer. *Aust. J. Chem.* **2003**, *56*, 1021–1024.
- (24) Johnson, B. K.; Prud'homme, R. K. Mechanism for rapid self-assembly of block copolymer nanoparticles. *Phys. Rev. Lett.* **2003**, *91*, 118302.
- (25) Liu, J.; Zeng, F.; Allen, C. In vivo fate of unimers and micelles of a poly(ethylene glycol)-block-poly(caprolactone) copolymer in mice following intravenous administration. *Eur. J. Pharm. Biopharm.* **2007**, *65*, 309–319.
- (26) Allen, T. M.; Hansen, C.; Martin, F.; Redemann, C.; Yau-Young, A. Liposomes containing synthetic lipid derivatives of poly(ethylene glycol) show prolonged circulation half lives in vivo. *Biochim. Biophys. Acta* **1991**, *1066*, 29–36.
- (27) Desai, N.; Trieu, V.; Yao, Z.; Louie, L.; Ci, S.; Yang, A.; Tao, C.; De, T.; Beals, B.; Dykes, P.; Noker, P.; Yao, R.; Labao, E.; Hawkins, M.; Soon-Shiong, P. Increased antitumor activity, intratumor paclitaxel concentrations and endothelial cell transport of cremophor-free, albumin bound paclitaxel, ABI-007, compared with Cremophor-based paclitaxel. *Clin. Cancer Res.* **2006**, *12*, 1317–1324.
- (28) Fetterly, G. J.; Straubinger, R. M. Pharmacokinetics of paclitaxel-containing liposomes in rats. *AAPS PharmSci* **2003**, *5*, 1–11.
- (29) Sparreboom, A.; Scripture, C. D.; Trieu, V.; Williams, P. J.; De, T.; Yang, A.; Beals, B.; Figg, M.; Hawkins, W. D.; Desai, N. Comparative preclinical and clinical pharmacokinetics of a Cremophor free, nanoparticle albumin-bound paclitaxel (ABI-007) and paclitaxel formulated in Cremophor (Taxol). *Clin. Cancer Res.* **2005**, *11*, 4136–4143.
- (30) Sparreboom, A.; van Zuylen, L.; Brouwer, E.; Loos, W. J.; de Bruijn, P.; Gelderblom, H.; Pillay, M.; Nooter, K.; Stoter, G.; Verweij, J. Cremophor EL-mediated alteration of paclitaxel distribution in human blood: clinical pharmacokinetic implications. *Cancer Res.* **1999**, *59*, 1454–1457.
- (31) Mosmann, T. Rapid colorimetric assay for cellular growth and survival: application to proliferation and cytotoxicity assays. *J. Immunol. Methods* **1983**, *65*, 55–63.

JM800002Y